PHYSICAL REVIEW B **87**, 201104(R) (2013)

Scaling of the Kondo zero-bias peak in a hole quantum dot at finite temperatures

O. Klochan,[1,*] A. P. Micolich,[1] A. R. Hamilton,[1] D. Reuter,[2] A. D. Wieck,[2] F. Reininghaus,[3] M. Pletyukhov,[3] and H. Schoeller[3]

[1]*School of Physics, University of New South Wales, Sydney NSW 2052, Australia*

[2]*Angewandte Festkörperphysik, Ruhr-Universität Bochum, D-44780 Bochum, Germany*

[3]*Institut für Theorie der Statistischen Physik and JARA - Fundamentals of Future Information Technology, RWTH Aachen, 52056 Aachen, Germany*

(Received 19 November 2012; published 14 May 2013)

We have measured the zero-bias peak in differential conductance in a hole quantum dot. We have scaled the experimental data with applied bias and compared to real-time renormalization group calculations of the differential conductance as a function of source-drain bias in the limit of zero temperature and at finite temperatures. The experimental data show deviations from the $T = 0$ calculations at low bias, but are in very good agreement with the finite-T calculations. The Kondo temperature T_K extracted from the data using $T = 0$ calculations, and from the peak width at $\frac{2}{3}$ maximum, is significantly higher than that obtained from finite-T calculations.

DOI: 10.1103/PhysRevB.87.201104 PACS number(s): 72.15.Qm, 73.63.Rt, 73.23.Ad, 73.63.Kv

The Kondo effect arises due to interaction of a single localized electron spin with a sea of delocalized electron spins,[1] and it was first observed through a nonmonotonic temperature dependence of the resistivity of a metal doped with magnetic impurities.[2] The strength of this interaction is characterized by a single parameter called the Kondo temperature T_K. In metals the Kondo effect is due to the contribution of many magnetic impurities, so it is interesting to ask, What happens in the case of a single impurity? This question was answered experimentally in low-temperature STM experiments[3] where individual Co atoms were placed at Au surface and were probed with an STM tip. Alternatively, a quantum dot can be used to study the Kondo effect.[4,5] Here, a single unpaired electron spin trapped in the dot interacts with spins of electrons in the source and drain resulting in a many-body state which enhances conductance through the dot at low temperature. The major advantage of a quantum dot is the ability to tune the Kondo temperature over a wide range by changing a bias on one of the gate electrodes forming the dot.[6]

The usual method for measuring T_K in a quantum dot is to study the temperature dependence of the conductance and compare to theory using an empirical expression with T_K as a fitting parameter.[7] Recently a much simpler technique has become available based on analyzing the conductance as a function of source-drain bias instead of temperature. The Kondo enhanced conductance is suppressed by a source drain bias V_{SD} across the dot, producing a characteristic peak in the differential conductance $G'(V_{SD})$, the zero-bias peak (ZBP). Recently,[8] a two-loop real-time renormalization group theory (RTRG) has been applied to a Kondo-$\frac{1}{2}$ model and provided numerical results for the bias dependence of differential conductance in the limit of zero temperature $T = 0$. These calculations have been used in recent experiments on InAs nanowires[9] to extract values of T_K and compare to the values obtained from the linear conductance measured as a function of temperature. Here we measure the zero-bias peak in differential conductance in a spin-$\frac{3}{2}$ hole quantum dot. We scale the zero-bias peak as a function of V_{SD} and compare to RTRG calculations in the limit of $T = 0$ and at finite T. We observe deviations between our experimental data and the $T = 0$ calculations[8] at low bias. We show that these deviations arise from the finite measurement temperature and can be taken into account by scaling the experimental data to newly available finite-T calculations.[10] These results suggest that the Kondo effect in a spin-$\frac{3}{2}$ GaAs hole quantum dot can be accurately described by a Kondo-$\frac{1}{2}$ model.

The system studied here is a hole quantum dot defined in the two-dimensional (2D) hole system at a GaAs-AlGaAs heterojunction. It is technically difficult to fabricate small hole quantum dots to access the single-hole regime due to the large hole effective mass ($m_h = 0.2$–$0.5 \times m_0$) and poor electrical stability of hole nanodevices.[13] Instead, we form a very small quantum dot in a quantum wire near pinch-off due to the roughness of the wet etching used to define the wire (see, e.g., Ref. 14). The wire is etched 20 nm deep through degenerately doped cap layer used to induce the carriers electrostatically, which results in rather stable devices.[15] Details of the fabrication can be found in Ref. 12. All measurements were taken in a dilution refrigerator at a top gate voltage $V_{TG} = -0.67$ V corresponding to a two-dimensional density $p = 2 \times 10^{11}$ cm^{-2} and mobility $\mu = 450\,000$ cm^2/V s.

It is not obvious that Kondo physics will be the same for holes as for spin-$\frac{1}{2}$ electrons, since holes in GaAs have a p-type wave function and nonzero orbital momentum l, giving a total angular momentum $j = l + s = \frac{3}{2}$. Holes have much stronger spin-orbit coupling, and very different spin properties, to electrons: In a two-dimensional hole system the fourfold degeneracy of the hole bands is split into two doubly degenerate bands with projections of $j = \pm\frac{3}{2}$ (heavy holes) and $j = \pm\frac{1}{2}$ (light holes). We work in the low-carrier density regime where only the heavy-hole band is occupied. The holes are then confined to lower dimensions using surface gates, which give a weaker confinement potential than the self-consistent triangular well at the heterointerface. This suggests that the nature of the hole states remains predominantly heavy-hole like. This is consistent with the anisotropy of the splitting of the one-dimensional subbands with in-plane field[11] being the same as the anisotropic response of the ZBP.[12] Therefore it is possible a Kondo-$\frac{1}{2}$ model can be applied, since the Kondo effect

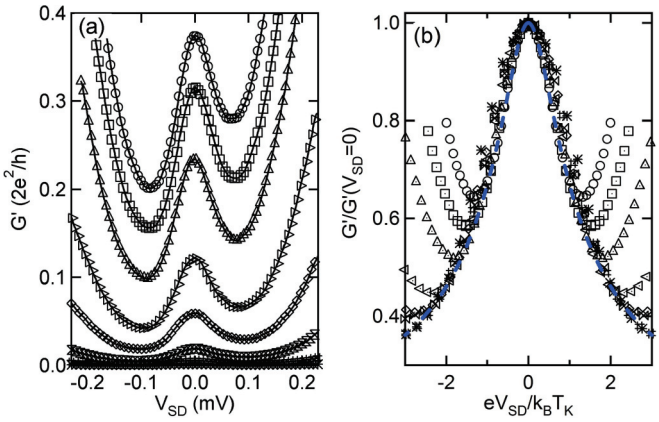

FIG. 1. (Color online) (a) Differential conductance G' below $0.4 \times 2e^2/h$ as a function of V_{SD} showing a pronounced ZBP for all traces. Top trace is measured at $V_{SG} = 1.08$ V, bottom trace at $V_{SG} = 1.115$ V, and the step size between adjacent traces is 5 mV. (b) Experimental data (symbols) from (a) symmetrized and scaled onto the universal trace for $T = 0$ (dashed blue line). For clarity only every 10th experimental data point is shown.

only requires a doubly degenerate level to facilitate transport, independently of the exact nature of the spin or pseudospin.

Figure 1(a) shows the differential conductance G' as a function of applied source drain bias[16] V_{SD} measured for a series of side-gate voltages V_{SG} corresponding to $10^{-3} < G'(V_{SD} = 0) < 0.4 \times 2e^2/h$. A clear zero-bias peak centered at $V_{SD} = 0$ V is present in all traces. It is important to note that the zero-bias peak reported here is distinct from the zero-bias anomaly observed in quantum wires. In quantum wires the zero-bias anomaly shows a linear splitting in magnetic field that is exponentially dependent on V_{SG}.[17,18] The zero-bias anomaly in electron quantum dots, and in the hole dot studied here, also splits with an applied magnetic field, but the splitting is independent of V_{SG}.[4,5,12]

Observation of the signatures of the Kondo effect in magnetic field[12] indicates that the dot is small enough to see Kondo physics, and that we sit in a single Kondo valley where the dot occupancy is odd.[19] The zero-bias peak in Fig. 1(a) is superimposed on a rising background, which has been attributed to charge fluctuations in the mixed-valence regime in quantum dots[7,23] or enhanced tunneling through a single barrier.[24] The conductance traces are asymmetric with respect to V_{SD} due to self-gating,[24] which we eliminate in our analysis by symmetrizing the experimental data with respect to $V_{SD} = 0$ V. We can estimate the Kondo temperature from the width of the zero-bias peak. The $T = 0$ theory[8,9] gives the full width at $\frac{2}{3}$ maximum as $\mathrm{FW2/3M} = 2T_K$. As we go down from the top trace to the bottom in Fig. 1(a), the conductance drops by almost three orders of magnitude whereas the FW2/3M does not change significantly. Because T_K depends exponentially on the coupling between the dot and the leads it should change drastically.[7] This implies that the dot is coupled asymmetrically to the leads with the more opaque barrier controlling the overall conductance while the more transparent barrier defines the Kondo temperature.[25] When the conductance exceeds e^2/h one of the barriers becomes completely transparent and we measure transport through a single barrier only; therefore to probe quantum dot physics we need to stay in the low-conductance regime below e^2/h. Thus the Kondo enhancement in these measurements cannot reach the unitary conductance limit $G_0 = 2e^2/h$.

We scale our data to numerically calculated $G'(V_{SD})$ in the limit of $T = 0$ using T_K as a single fitting parameter,[8] following a similar procedure to Ref. 9. To account for the asymmetric barriers we first normalize each ZBP trace by its zero-bias value $G'(V_{SD} = 0)$ to obtain $G'/G'(V_{SD} = 0)$ (even when the system is asymmetric this procedure is still valid as shown previously,[8,9] since the fit is primarily driven by the steepness of the conductance drop with applied source drain bias). Second, we plot both the experimental and the calculated $G'(V_{SD})/G'(V_{SD} = 0)$ as a function of scaled bias eV_{SD}/k_BT_K on a semilog scale. Third, we shift each experimental trace along the eV_{SD}/k_BT_K axis (adjust T_K) until it overlaps with the theoretical curve (because the ZBP is superimposed onto the rising background, the experimental data should always be above the calculations, particularly at large biases). The value of the shift required to make the experimental and calculated traces overlap then gives T_K.

The results of scaling are presented in Fig. 1(b). Note that although the scaling is performed on a semilog scale, the scaled data are shown on a linear scale to highlight the ZBP. At first sight the scaling of the experimental data (black symbols) to the calculated trace for $T = 0$ (blue dashed line) looks very good, apart from the upturn due to the rising background in the experimental data at high bias ($eV_{SD}/k_BT_K > 1$). However, closer inspection of Fig. 1(b) reveals that the experimental data are consistently above the $T = 0$ calculations in the low-bias window $|eV_{SD}/k_BT_K| < 1$, where the agreement between theory and experiment should be best. An example of this is shown in Fig. 2(a), where a single experimental

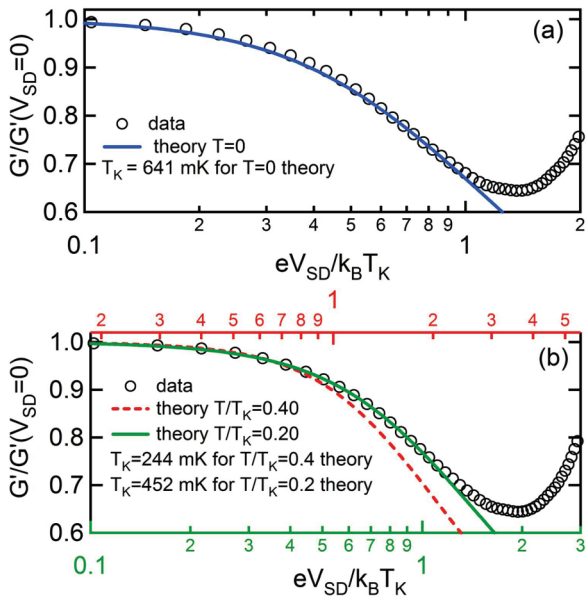

FIG. 2. (Color online) (a) An experimental trace at $V_{SG} = 1.08$ V (symbols) compared with the calculated traces for $T/T_K = 0$ (solid blue line). (b) The same experimental data compared with finite temperature calculations for $T/T_K = 0.20$ (green solid line, bottom x axis) and $T/T_K = 0.4$ (red dashed line, top x axis). For clarity only every 5th experimental data point is shown.

trace measured for $V_{SG} = 1.08$ V [the top trace in Fig. 1(a)] is fitted to the $T = 0$ theory using T_K as the only adjustable parameter. We can see that the experimental data lie above the theory for most of the low-bias region. The fact that our data in Fig. 2(a) deviate from the calculated trace for $T = 0$ suggests that the measurements are not in the low-T/T_K limit. Previous experiments[23] which showed good agreement between the $T = 0$ theory and experiment were performed in a system with $T/T_K < 0.03$. In contrast, we performed experiments on a system with smaller T_K and higher measurement temperature so that we can reach higher T/T_K.

The RTRG calculations of the differential conductance $G'(eV_{SD}/k_BT_K, T/T_K)$ in Ref. 8 only consider the limiting cases where either the bias voltage V_{SD} or the temperature T are zero. Very recently[10] it has become possible to extend these calculations so that $G'(eV_{SD}/k_BT_K, T/T_K)$ can be computed for all V_{SD} and T. We have used 21 numerically calculated traces of $G'(eV_{SD}/k_BT_K, T/T_K)$ in the range $0 < T/T_K < 0.8$ in steps of 0.04 to find the best fit to each of our experimental traces. To demonstrate the improved agreement between the finite-T theory and the experimental data we show different calculated traces fitted to a single experimental trace in Fig. 2(b). We recall that the calculations for $T/T_K = 0$ in Fig. 2(a) lie below the experimental data, because the ratio $T/T_K = 0$ is too small to produce a good fit—on the semilog axes of Fig. 2(a) changing T_K only shifts the experimental data sideways, without altering the slope of the curve. In Fig. 2(b) the same experimental data are plotted against both the top (red) the bottom (green) x axis, along with the optimal theory calculations for $T/T_K = 0.2$ (green solid line, bottom x axis) and $T/T_K = 0.4$ (red dashed line, top x axis). Note that the experimental data in Fig. 2(b) can be read off either top or bottom axes, since T_K is different for the experimental data when comparing with the two theoretical traces. For $T/T_K = 0.20$, we find very good agreement over the entire bias range, and extract $T_K = 452 \pm 50$ mK. Increasing T/T_K to 0.4 (red dashed line, top x axis) fits the experiment well for $eV_{SD}/k_BT_K < 0.4$ but deviates significantly at higher biases, indicating that the ratio $T/T_K = 0.4$ is too high. The error in T_K is estimated by fitting the experimental trace to the two traces on each side of the optimal ratio and taking the average of the extracted T_K.

We perform the same fitting procedure for different side gate voltages, as shown in Fig. 3. We consistently get a better fit of experiment to theory when using calculations for $T/T_K > 0$ (solid green lines, bottom x axis), compared to $T/T_K = 0$ (dashed blue lines, top x axis). Using the values of T/T_K and T_K obtained from Figs. 2(b) and 3 we can estimate the hole temperature T for each of the experimental traces. We obtain $T = 85 \pm 5$ mK consistent with the temperature obtained by analyzing Shubnikov–de Haas oscillations from a GaAs two dimensional hole system performed in the same setup.

In Fig. 4 we compare the values of T_K obtained from fitting to the $T/T_K = 0$ and $T/T_K > 0$ theory with those obtained from the peak width at $\frac{2}{3}$ maximum. From the shape of the universal $G'(V_{SD}, T_K)/G_0$ conductance trace obtained from the $T = 0$ theory [blue line in Fig. 1(b)], it can easily be seen that $G'/G_0 = 0.67$ occurs at $eV_{SD} = T_K$. Therefore the values of T_K obtained from FW2/3M (black triangles) and the complete $T/T_K = 0$ fit (blue squares) in Fig. 4 should coincide as long as T/T_K is small. We can see in Fig. 4 that both traces follow the same trend, although the two traces separate from each other at larger V_{SG}, where T_K is small. This is because the $T = 0$ theory does not fit the experimental data

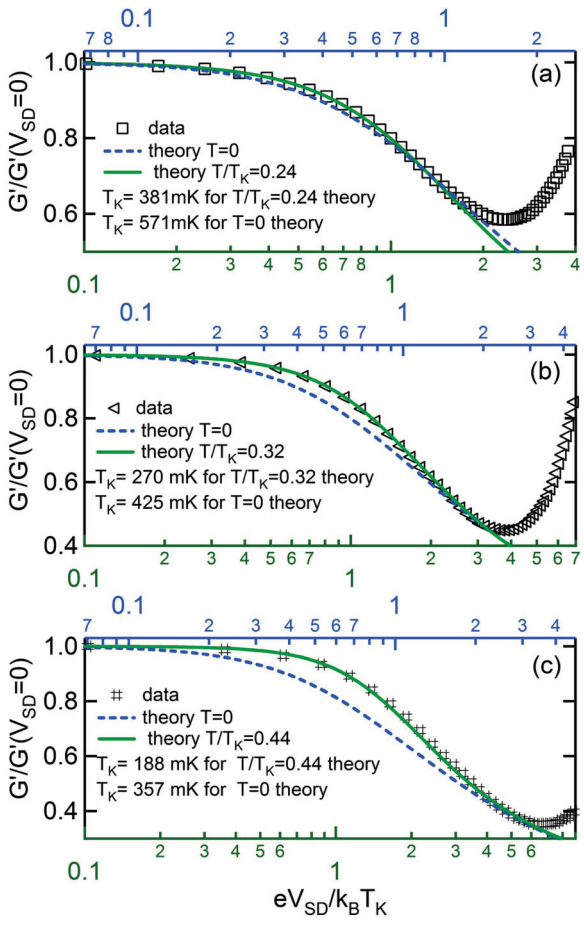

FIG. 3. (Color online) Experimental conductance data (symbols) compared with theoretical fits for $T/T_K = 0$ (blue dashed line, top x axis) and $T/T_K > 0$ (green solid line, bottom x axis) in the low-bias regime. (a) $V_{SG} = 1.085$ V, (b) $V_{SG} = 1.095$ V, and (c) $V_{SG} = 1.11$ V. For clarity only every 5th experimental data point is shown.

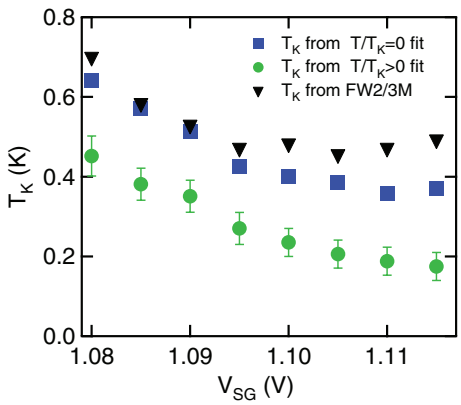

FIG. 4. (Color online) The values of T_K extracted from the fit of experimental data to $T = 0$ calculations (blue squares), $T/T_K > 0$ calculations (green circles), and FW2/3M (black triangles) as a function of V_{SG}.

well in this regime (see Fig. 3). Furthermore, both FW2/3M and the $T/T_K = 0$ fit significantly overestimate the value of the real T_K obtained from fitting to the finite-T theory (green circles). This shows that the zero-bias peak width cannot be used as an accurate estimate of the Kondo temperature at finite measurement temperatures.

To conclude, we have measured the zero-bias peak in differential conductance in a hole quantum dot. We have scaled the experimental data and compared it to real-time renormalization group calculations of differential conductance as a function of source-drain bias in the limit of zero temperature T and at finite temperatures. Our experimental data show deviations from the $T = 0$ calculations at low bias and are in very good agreement with the finite-T calculations. The Kondo temperature T_K obtained from fitting the data to finite-T calculations is significantly lower than that extracted from the peak width at $\frac{2}{3}$ maximum and $T = 0$ calculations.

This work was funded by the Australian Research Council through the DP, FT, APF, and DORA schemes. Three co-authors (F.R, M.P., and H.S.) acknowledge financial support from the DFG via the project FOR 723.

*klochan@phys.unsw.edu.au

[1] J. Kondo, Prog. Theor. Phys. **32**, 37 (1964).

[2] W. J. de Haas, J. de Boer, and G. J. Van den Berg, Physica **1**, 1115 (1933).

[3] V. Madhavan, W. Chen, T. Jamneala, M. F. Crommie, and N. S. Wingreen, Science **280**, 567 (1998).

[4] D. Goldhaber-Gordon, H. Shtrikman, D. Mahalu, D. Abusch-Magder, U. Meirav, and M. A. Kastner, Nature (London) **391**, 156 (1998).

[5] S. M. Cronenwett, T. H. Oosterkamp, and L. P. Kouwenhoven, Science **281**, 540 (1998).

[6] L. P. Kouwenhoven and L. I. Glazman, Phys. World **14**, 33 (2001).

[7] D. Goldhaber-Gordon, J. Göres, M. A. Kastner, Hadas Shtrikman, D. Mahalu, and U. Meirav, Phys. Rev. Lett. **81**, 5225 (1998).

[8] M. Pletyukhov and H. Schoeller, Phys. Rev. Lett. **108**, 260601 (2012).

[9] A. V. Kretinin, H. Shtrikman, and D. Mahalu, Phys. Rev. B **85**, 201301(R) (2012).

[10] F. Reininghaus, M. Pletyukhov, and H. Schoeller (unpublished).

[11] J. C. H. Chen, O. Klochan, A. P. Micolich, A. R. Hamilton, T. P. Martin, L. H. Ho, U. Zülicke, D. Reuter, and A. D. Wieck, New J. Phys. **12**, 033043 (2010).

[12] O. Klochan, A. P. Micolich, A. R. Hamilton, K. Trunov, D. Reuter, and A. D. Wieck, Phys. Rev. Lett. **107**, 076805 (2011).

[13] K. Ensslin, Nat. Phys. **2**, 587 (2006).

[14] F. Sfigakis, C. J. B. Ford, M. Pepper, M. Kataoka, D. A. Ritchie, and M. Y. Simmons, Phys. Rev. Lett. **100**, 026807 (2008).

[15] O. Klochan, W. R. Clarke, R. Danneau, A. P. Micolich, L. H. Ho, A. R. Hamilton, K. Muraki, and Y. Hirayama, Appl. Phys. Lett. **89**, 092105 (2006).

[16] A series resistance of ≈30.5 kΩ due to ohmic contacts is used to calculate the voltage drop across the dot.

[17] S. M. Cronenwett, H. J. Lynch, D. Goldhaber-Gordon, L. P. Kouwenhoven, C. M. Marcus, K. Hirose, N. S. Wingreen, and V. Umansky, Phys. Rev. Lett. **88**, 226805 (2002).

[18] S. Sarkozy, F. Sfigakis, K. Das Gupta, I. Farrer, D. A. Ritchie, G. A. C. Jones, and M. Pepper, Phys. Rev. B **79**, 161307(R) (2009).

[19] If the dot occupancy were even, the Kondo effect could also arise due to single-triplet degeneracy which can be tuned either by magnetic field (Ref. 20) or confinement potential (Ref. 21). However, the even Kondo effect is characterized by nonmonotonic dependence of the ZBP in magnetic field and temperature (Ref. 22). We do not observe these signatures. Moreover in our device, the splitting of the ZBP in magnetic field is double the Zeeman energy, which is only expected for odd dot occupancy (Ref. 12).

[20] S. Sasaki, S. De Franceschi, J. M. Elzerman, W. G. van der Wiel, M. Eto, S. Tarucha, and L. P. Kouwenhoven, Nature (London) **405**, 764 (2000).

[21] A. Kogan, G. Granger, M. A. Kastner, D. Goldhaber-Gordon, and H. Shtrikman, Phys. Rev. B **67**, 113309 (2003).

[22] G. Granger, M. A. Kastner, I. Radu, M. P. Hanson, and A. C. Gossard, Phys. Rev. B **72**, 165309 (2005).

[23] A. V. Kretinin, H. Shtrikman, D. Goldhaber-Gordon, M. Hanl, A. Weichselbaum, J. von Delft, T. Costi, and D. Mahalu, Phys. Rev. B **84**, 245316 (2011).

[24] L. Martin-Moreno, J. T. Nicholls, N. K. Patel, and M. Pepper, J. Phys.: Condens. Matter **4**, 1323 (1992).

[25] M. Pustilnik and L. Glazman, J. Phys.: Condens. Matter **16**, R513 (2004).